SWIFT: Spectroscopic WIde Field Telescope

A. Dey, J. Najita, G. Jacoby, C. Claver, S. Barden, C. Harmer
NOAO

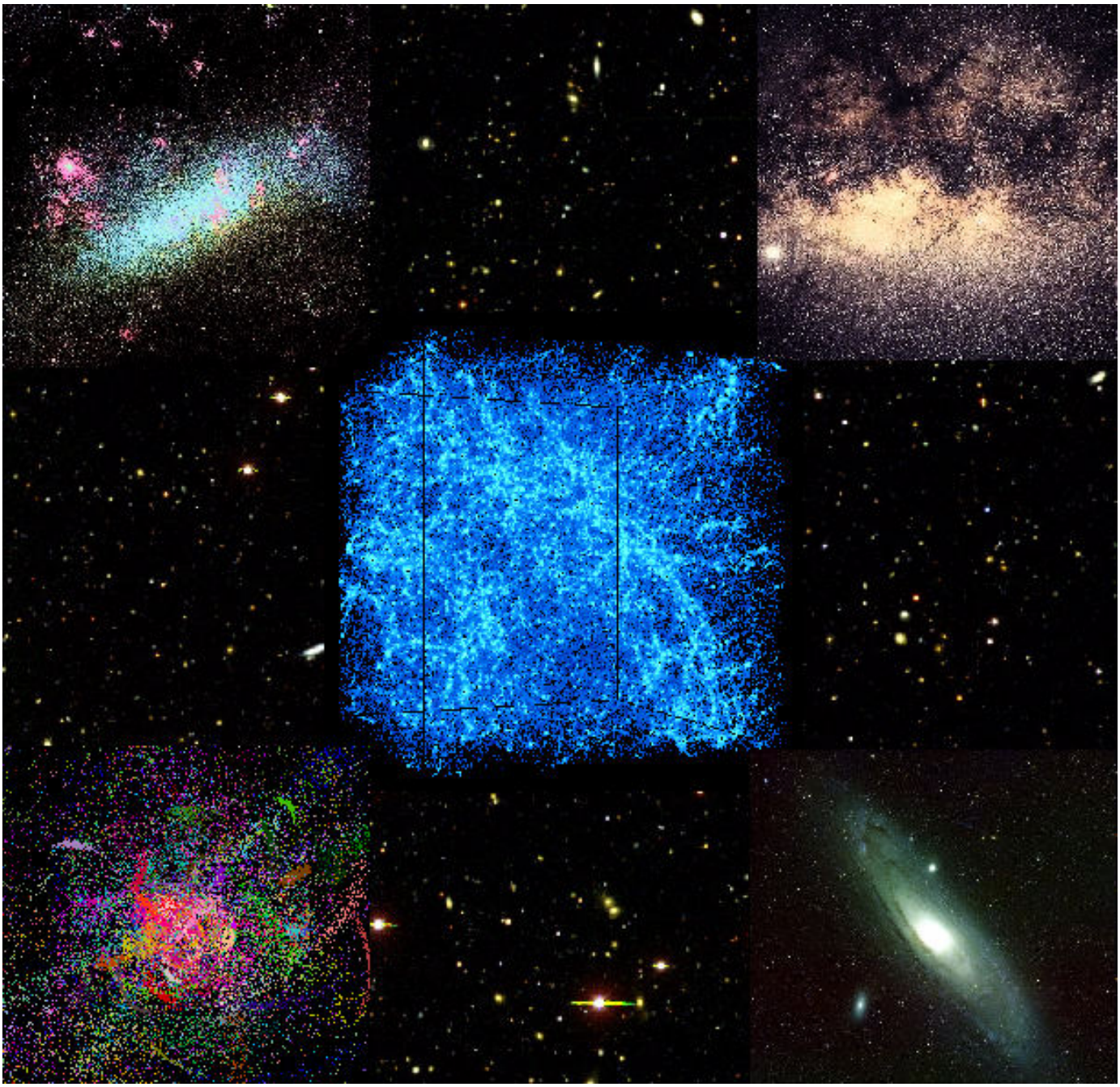

Contents

List of Tables

Cover Figure: The galaxy field shown in the background is an 800″ $B_W RI$ image from the NOAO Deep Wide-Field Survey; the survey will eventually cover a total of 18□° (Jannuzi & Dey 1999). The central figure shows the simulated 3D structure of the Universe at $z = 3$ in a CDM model with a cosmological constant; the box is 30 h^{-1} Mpc on a side (A. Klypin, personal communication). The other four images are (clockwise from upper left): the LMC (ROE/AAO); the Milky Way (AAO); Andromeda (NOAO/NSF); and simulated halo streamers from the "Spaghetti project" (P. Harding, personal communication).

1. A SPECTROSCOPIC FACILITY FOR THE NEW MILLENIUM

At the approach of the new millenium, we are poised at the threshold of addressing fundamental astrophysical questions about the origin and evolution of the Universe and its contents. The confluence of technological advances in telescope and spectrograph design; rapid growth in computing power; pathfinding imaging surveys on the ground and in space; and increasingly sophisticated theories of structure formation and the evolution of galaxies have inspired us to look beyond the study of a few unique objects to the systematic investigation of large samples in order to pin down their global physical properties, their formation and evolutionary history, and their cosmological significance.

In this document we argue that a National facility optimized for highly multiplexed multi-object spectroscopy is the missing element that is needed to realize this goal. We propose to develop a spectroscopic system with an integrated telescope and spectrograph design that achieves deep (22–26 mag), high-throughput, highly multiplexed (2,000-10,000 objects) spectroscopy over a wide field (1.5°) at optical and near-infrared wavelengths. This facility, SWIFT, will enable spectroscopy that is nearly two orders of magnitude more efficient than that provided by extant or planned facilities. These spectroscopic observations will probe the kinematics, chemical compositions, dynamics, ages, masses, evolutionary histories ... the very *nature* of astronomical objects.

The highly multiplexed multi-object spectroscopic capability of this facility will allow astronomers to contemplate and carry out ground-breaking investigations of a more mature character, larger scope, and more comprehensive nature than have been possible to date. The large-scale science enabled by SWIFT complements the high-angular-resolution science targeted by existing 8-m and 10-m class telescopes.

In the following section (§2), we discuss global astrophysical issues (large scale structure, galaxy evolution, and Galactic structure) that drive a spectroscopic need that is not met by any existing or planned instruments at large aperture telescopes. We then briefly describe the recent rapid growth in ground-based (§3) and space-based imaging capabilities (§4) that similarly require an efficient spectroscopic capability in order to achieve their astrophysical goals. Section 5 describes SWIFT, one such facility (the telescope, spectrograph, and ancillaries) which would meet this need, and compares its capabilities with those available (or soon to be) at the new generation of large aperture telescopes.

2. SWIFT SCIENCE

The story of our origins, begun in the crucible of the Big Bang, is largely a story of the evolution of structure and the chemical enrichment of the Universe. Beginning with the pioneering studies of galaxies in the 1920s, a host of pathfinding observations and theoretical predictions have led to the current version of this tale. At early epochs, the seeds of large structures, as fossilized in the cosmic microwave background radiation, begin to grow into the gigantic walls and voids manifest in the present-day galaxy distribution. As these initial perturbations grow, baryons accumulate in potential wells which eventually detach themselves from the universal expansion and collapse to form the first luminous stellar systems in the Universe. These fragmentary systems interact and merge to form increasingly larger systems, resulting in the galaxies that inhabit the present-day Universe. This hierarchical process of galaxy formation and evolution is a dynamic one, occurring between redshifts of 10 to 1 for the more massive systems, and at lower redshifts for the less luminous dwarfs. In this picture, the bulk of the stellar populations that comprise luminous galaxies such as the Milky Way were likely formed at redshifts beyond 1, i.e., more than 6 Gyr ago.

While this picture serves as a useful guide, many aspects are currently so poorly constrained that its applicability to the real Universe is difficult to judge. The detailed astrophysical processes that govern the formation and evolution of galaxies and determine their properties are largely unstudied: current observations provide only the crudest glimpse of the star formation, metal enrichment and dynamical merging history of the present day galaxies. In addition, the cosmological parameters that determine the geometry and expansion rate of the Universe and directly affect the formation and evolution of structure are still uncertain, as is the relationship between the initial density fluctuation spectrum and the observed large scale structure traced by luminous objects. Finally, the processes which govern star formation in a variety of environments and enrich the Universe with heavy elements, both in galaxies and in intergalactic space, remain largely in the realm of theoretical debate.

Unambiguously resolving these issues requires a highly multiplexed multi-object capability such as SWIFT. These issues can be addressed both by direct observations of millions of galaxies spread out over cosmic time, and by detailed study of the history of the Milky Way and its neighbors, as maintained in the fossil record of galactic stars. In this section, we describe a small sample of programs that SWIFT will enable astronomers to contemplate and carry out in order to address these issues. There are clearly many more.

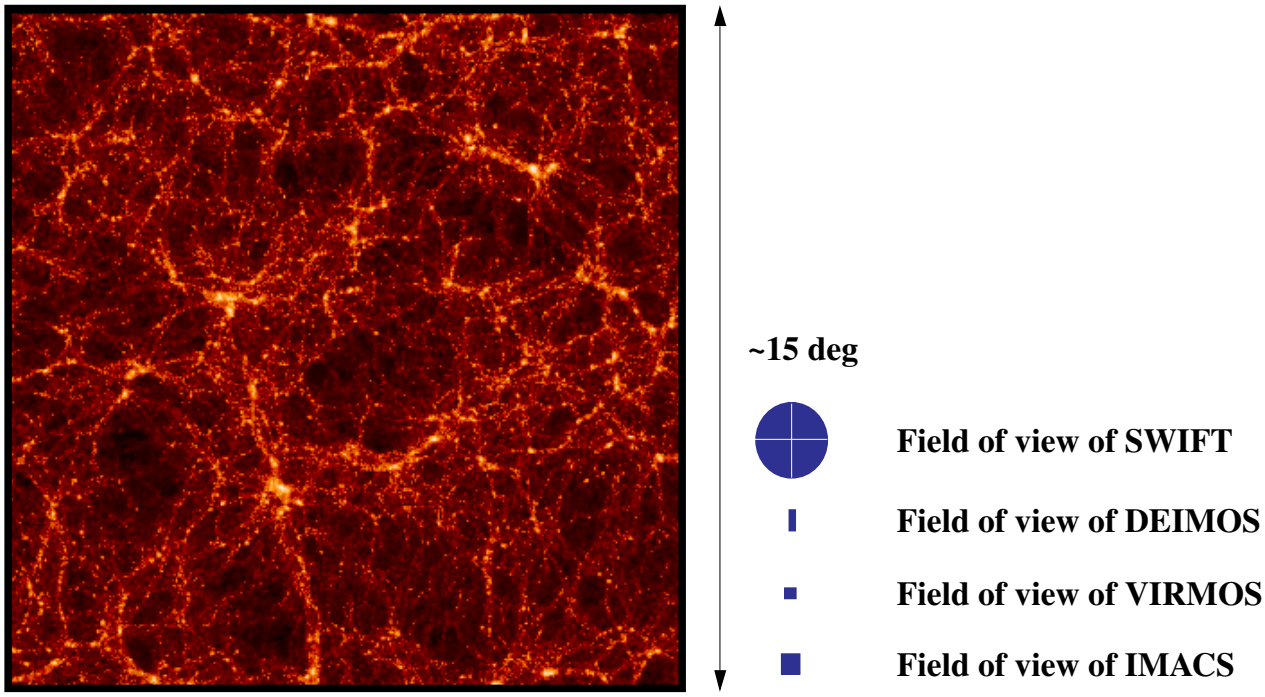

Fig. 1.— Numerical simulations of the dark matter distribution predict structures on scales of clumps and filaments (arcminutes) to large voids and walls (several degrees). Characterizing this structure from observations of galaxy clustering requires a wide-field, highly multiplexed spectroscopic capability.

2.1. The Growth of Structure

One of the most important problems in astrophysics is understanding how structures in our Universe have evolved from the tiny spatial fluctuations observed in the cosmic microwave background to the clumpy and highly non-Gaussian matter distributions that we observe today. Thus far, our understanding of structure formation, lacking comprehensive observational data, has been largely guided by theoretical studies. Numerical simulations of structure formation have now attained a high degree of sophistication, and demonstrate that clear differences between competing cosmological structure formation models may be observable at large lookback times ($z \sim 1-5$; figure 2). Confronting these models with observations of the matter distribution at a range of lookback times remains one of the most robust methods of discriminating between present competing models and constraining future theories of structure formation. This requires obtaining redshifts for galaxies over very large areas of the sky (to probe the characteristic scales on which structures exist) to very faint limiting magnitudes (to probe the distant universe). Redshift surveys would not

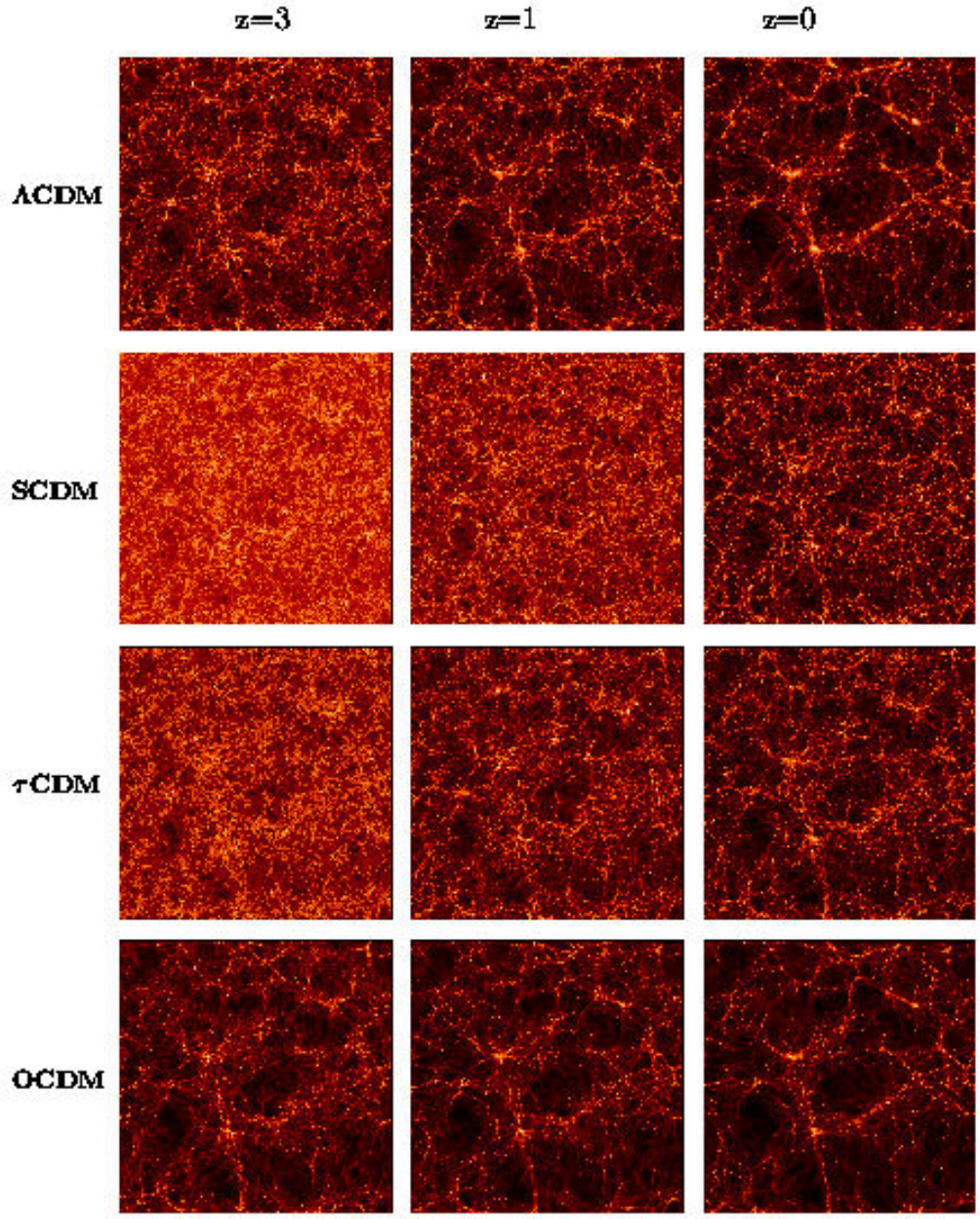

Fig. 2.— In numerical simulations of the growth of large scale structure, differences between competing models are especially obvious at large lookback times. In these simulations from the VIRGO Consortium (e.g., White 1997), the boxes ($240h^{-1}$Mpc on a side, corresponding to $\sim 15°$ at $z = 1$) show the dark matter distributions at different epochs and predict discernible differences at $z > 1$.

only probe the overall topology of the matter distribution, but also the detailed dynamical history of galaxies in a variety of environments from the sparse voids to the densest clusters.

Need for Large Area / Depth / Large Samples: Current surveys suggest that there is significant structure on $\sim 100h^{-1}$ Mpc scales (corresponding to $\sim 6^\circ$ at z=1), comparable to the largest scales thus far investigated (e.g., Landy et al. 1996, Doroshkevich et al. 1996). The mass distribution may be comprised of large filamentary or sheet-like structures which are inferred from pencil-beam surveys — little is known about the true large scale angular distribution at each epoch due to the paucity of redshift information over large angular scales for all but the very nearest galaxies ($z \lesssim 0.2$; e.g., Davis et al. 1982, Shechtman et al. 1996, Ellis et al. 1996, Geller et al. 1997, da Costa et al. 1998). This implies the need for spectroscopic surveys over several times this characteristic scale (i.e., $\gtrsim 10^\circ \times 10^\circ$) in order to sample the large volumes that contain these structures (e.g., Figures 1 and 2).

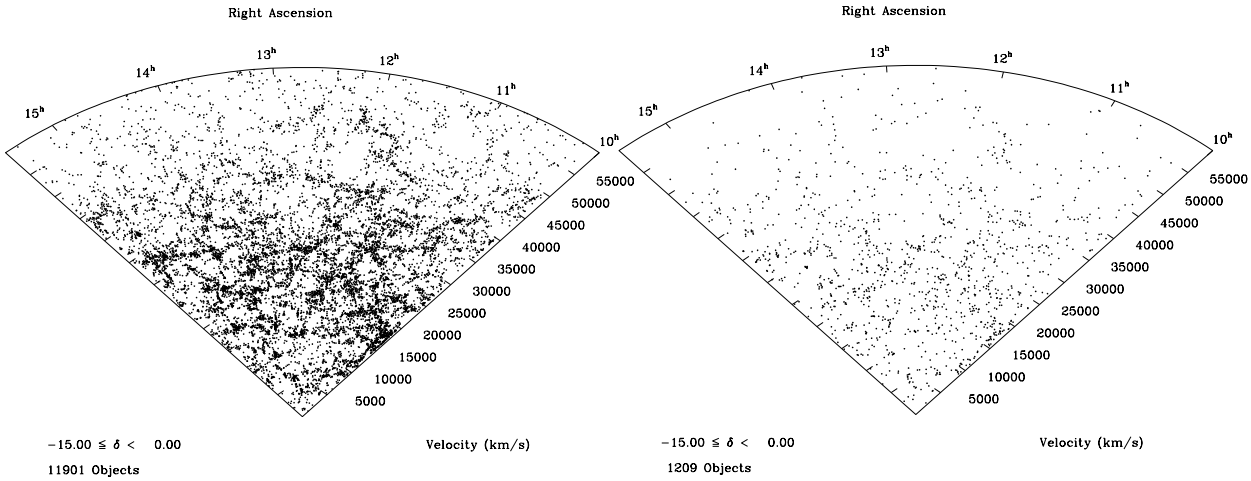

Fig. 3.— The need for dense sampling: when all the galaxies in the Las Campanas Redshift Survey (Left) are sampled at 10% (Right), the strongest features disappear.

A deep survey ($R \sim 25$AB) is needed to densely sample the high redshift populations and characterize the three-dimensional matter distribution to redshifts beyond 4. Dense sampling is needed to detect and highlight compact structures: most existing surveys of the sky are non-contiguous and sparsely sample the galaxy distribution. Sparse sampling is insensitive to strong clustering (Figure 3) and results in significant uncertainties in the derived structure statistics due to both sampling and 'cosmic' errors (e.g., Szapudi & Colomb 1996, Szapudi & Szalay 1996). Since the simulations show structures on scales ranging from tens of kpc to $\sim$ 100 Mpc, the observations must be sensitive enough to

sample the velocity fields on small and large scales, as well as comprehensive enough to have sufficient numbers of objects on all scales in each redshift interval to provide robust statistical measures of the spatial structures.

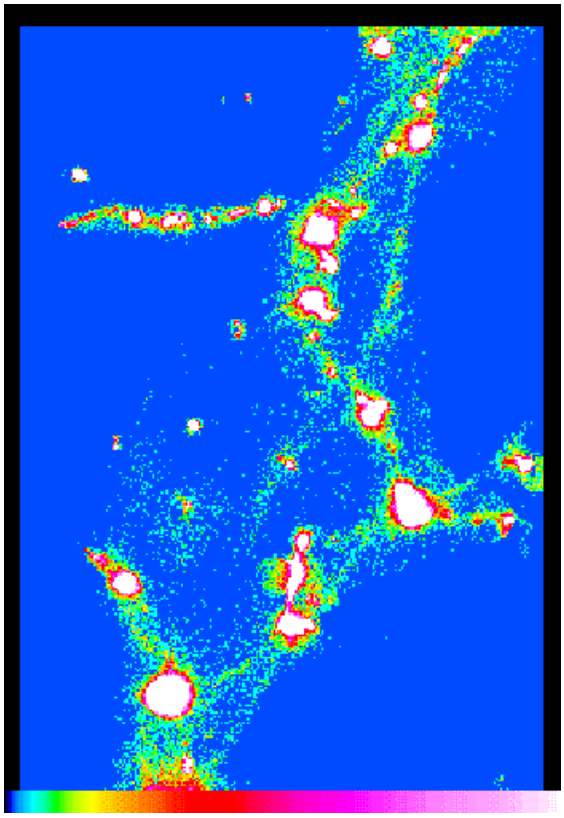

Fig. 4.— Simulation by M. Pierre (1998) of an XMM observation of an X-ray emitting filament located between two z=0.5 clusters (not shown). By measuring the velocities of galaxies in the different regions, SWIFT will locate the filaments and clumps in velocity space and measure the total mass in the virialized regions. The region shown is $\simeq 1.25° \times 1.82°$, and is well matched to the FOV of SWIFT.

A Representative SWIFT Project

To study the growth of structure from $z \simeq 4$ to $z \simeq 1$, we would map out galaxy redshifts over $\sim 10° \times 10°$. Dividing the redshift range crudely into 10 bins of $\delta z = 0.3$, and requiring $\sim 10^3$ galaxies/$\Box°$/δz bin for an accurate estimate of a clustering statistic, we would need a total sample size of about 10^6 galaxies. To $R \sim 25$AB mag, the surface density of galaxies is $10^5/\Box°$, the majority of which lie at $z > 1$. This program will reveal the evolution of the matter distribution as traced by the galaxies as a function of redshift, and provide a relatively unbiased discovery tool for high redshift clusters and groups. An investigation of the velocity fields of galaxies in regions imaged at X-ray wavelengths (e.g., figure 4) will isolate the hot X-ray emitting gas in redshift space, determine the fractional baryonic mass in galaxies versus that in hot gas, and provide a direct measure of the ratio of baryonic to total mass in filaments and clusters. Measuring redshifts of $\sim 10^6$ galaxies at a resolution $\lambda/\Delta\lambda \simeq 500$ requires 200 clear nights with SWIFT, whose field of view is well matched to the angular scale of structures predicted from simulations (figure 1). The efficiency gain

Table 1: Comparison of Completion Times for Some Science Projects

Program	m AB mag	N_{obj} /sq.deg.	N_{tot}	Keck+DEIMOS (nights)	IMACS (nights)	SWIFT (nights)
Large-scale Structure	25	10^5	10^6	12,500	4,000	200
Galaxy Evolution	25	10^4	5×10^5	6,250	1,975	100
Virgo Intracluster	"29"	$> 10^3$	10^5	4,500	1,000	100
Galactic Plane KIII	23	$\gtrsim 10^3$	4×10^5	18,000	4,700	225

compared with other large telescopes with MOS capability is shown in table 1.

In addition to mapping out the evolution of the large-scale topology of the matter distribution, a project of this scale would simultaneously yield detailed dynamical information on clusters of galaxies over a large range in redshift. Since the densest clusters identify sites of the strongest initial perturbations and the earliest ones to collapse, interactions play an important role in shaping the evolution of galaxies in clusters and perhaps in the chemical and stellar enrichment of the inter-cluster medium as a whole. The dynamical analysis of member galaxies in clusters at high redshift, when combined with detailed kinematic and chemical studies of galaxies and intracluster stars and gas in clusters at the present epoch, can yield a comprehensive understanding of the chemical enrichment of the Universe in these over-dense regions. In particular, the intracluster stellar component in nearby clusters contains a fossil record of the past dynamical history imprinted in the kinematics of the intra-cluster stellar population. A chemical and kinematic study of the intra-cluster planetary nebulae (a good velocity tracer population that is relatively easy to identify from the ground) in these clusters, would reveal the entire tidal history of many cluster galaxies over the evolutionary history of the clusters! For example, the areal density of intracluster planetaries in Virgo (with line fluxes F([OIII]λ5007) $> 10^{-17}\,\mathrm{erg\,s^{-1}\,cm^{-2}}$) is $\simeq 1000/\Box^\circ$, and the cluster spans an area of $\sim 100\Box^\circ$. Obtaining moderate resolution, moderate signal-to-noise ratio spectra of $\simeq 10^5$ planetaries requires ~ 100 nights with SWIFT.

2.2. Formation and Evolution of Galaxies

How do galaxies form and evolve? Primeval galaxies undergoing their first episodes of star formation have remained elusive, either because these nascent systems are shrouded in dust or because galaxy formation is a slow hierarchical process wherein galaxies are assembled over time from small building blocks. The aging of galaxies has also remained a puzzle: so many factors contribute to the chemical, dynamical and morphological development of a galaxy, that the small observational data sets painstakingly obtained barely provide us with clues even to the most global issues (e.g., the evolution of the luminosity function) over a large range in lookback time.

Our investigation of the processes of galaxy formation and evolution is currently restricted to theoretical simulations and small observational data sets. Current simulations suggest that galaxy assembly is a hierarchical process, wherein mergers and interactions play a significant role in determining the present-day morphologies and stellar constituents of galaxies. At present, the observational data are ambiguous, and results suffer from selection effects and small number statistics. The pioneering studies during the last decade have been largely restricted to small pencil beam surveys or shallow surveys of the low-redshift galaxy population (e.g., CFRS - Lilly et al. 1996; LDSS/Autofib - Ellis et al. 1996; various Keck surveys - Cowie et al. 1996, Koo et al. 1996, Cohen et al. 1999). More recently, observations with *HST* and the Keck telescopes have demonstrated the existence of star-forming galaxies at redshifts beyond 3 (Steidel et al. 1996, 1999). These galaxies are believed to be the building blocks of the present-day galaxies, but their properties (masses, chemical composition, stellar content, ages and evolutionary histories) are almost completely unknown.

In order to address the question of galaxy formation and evolution for the entire population, we would ideally want to trace the evolutionary history of galaxies (i.e., their star-forming history, chemical evolution, merging and morphological evolution) as a function of mass, redshift and environment. It is critical to understand and interpret the formation of galaxies in the context of structure formation and evolution. These astrophysical problems are inextricably linked, since the large-scale environment plays a crucial role both in the assembly of galaxies and in their evolution (through merging, exclusion, harassment, etc.).

Need for Large Area / Depth / Large Samples: To trace the evolutionary history of galaxies as a function of environment, we need to sample galaxies over the entire range of environments: from the lowest density regions (voids) to the rarest high-density environments (cores of rich clusters). Surveys over large volumes ($\sim$100$\square^\circ$ — see previous section) are needed to accomplish this.

In order to explore the early evolutionary history of galaxies ($z \sim 4-6$), deep spectroscopic surveys (to ~ 25 AB mag) are essential. These depths are needed not only to probe the highest redshifts, but also to ensure that the samples are not restricted to the rarest, most luminous objects, and instead sample more typical objects as well (i.e., as much of the luminosity function as possible).

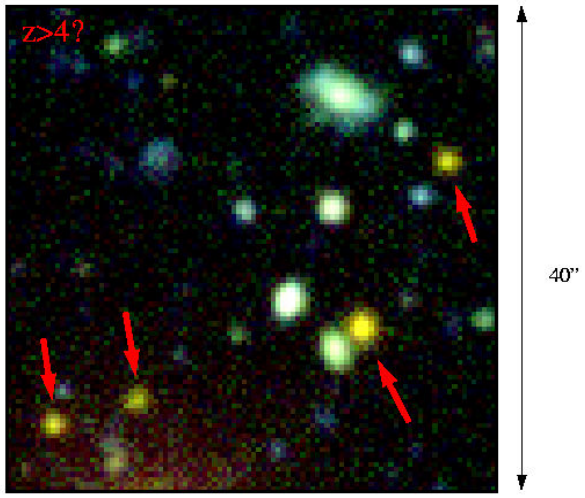

Fig. 5.— Deep, wide-field imaging surveys are recovering a high density of distant galaxy candidates. Spectroscopic follow-up is critical for an understanding of their stellar content, internal dynamics, chemistry, and evolutionary history. This B_W, R, I image is a postage stamp from the 18□° NOAO Deep Wide Field Survey showing a high density of $z > 4$ candidate galaxies (Jannuzi & Dey 1999).

Galaxies in the present epoch exhibit a large range in physical properties (e.g., masses, chemical abundances, star forming histories, morphologies, gas and stellar content). Since the evolutionary processes responsible for these properties are numerous and complex (e.g., star formation, mergers and interactions, infall), an obserational program to unravel the formation histories of present-day galaxies inherently requires large samples ($\sim 10^6$ galaxies). For example, in order to trace the evolutionary history of galaxies as a function of mass, redshift and environment, we would need at least 5 redshift bins ($1 < z < 6$), 4 mass bins (logarithmic intervals spanning $10^8 - 10^{12}\,M_\odot$), 5 bins in mean stellar age or star-formation rate (0.1 - 10Gyr or $0 - 10^3\,M_\odot/yr$), 4 bins in morphology (E/S0, S, Irr, multi-component), 4 bins in mean chemical abundance ($0.002 - 2Z_\odot$), and 3 bins in environmental density (field, groups, clusters). With at least 100 galaxies per bin, this implies a total sample size of at least 500,000 galaxies. This is truly a lower limit since we have required that the bins of rare objects are also well populated. Populating such rare bins is critical in order to address questions such as the formation history of the most massive galaxies, or the evolutionary history of the most metal-poor galaxies.

A Representative SWIFT Project

The surface densities on the sky of $R < 25$AB mag $z \approx 3$ and $I < 25$AB mag $z \approx 4$ galaxies are ≈ 4000 and 800/□° respectively. A survey of 5×10^5 galaxies over 100□° requires a wide-field, highly multiplexed multi-object capability. We are only beginning to scratch the

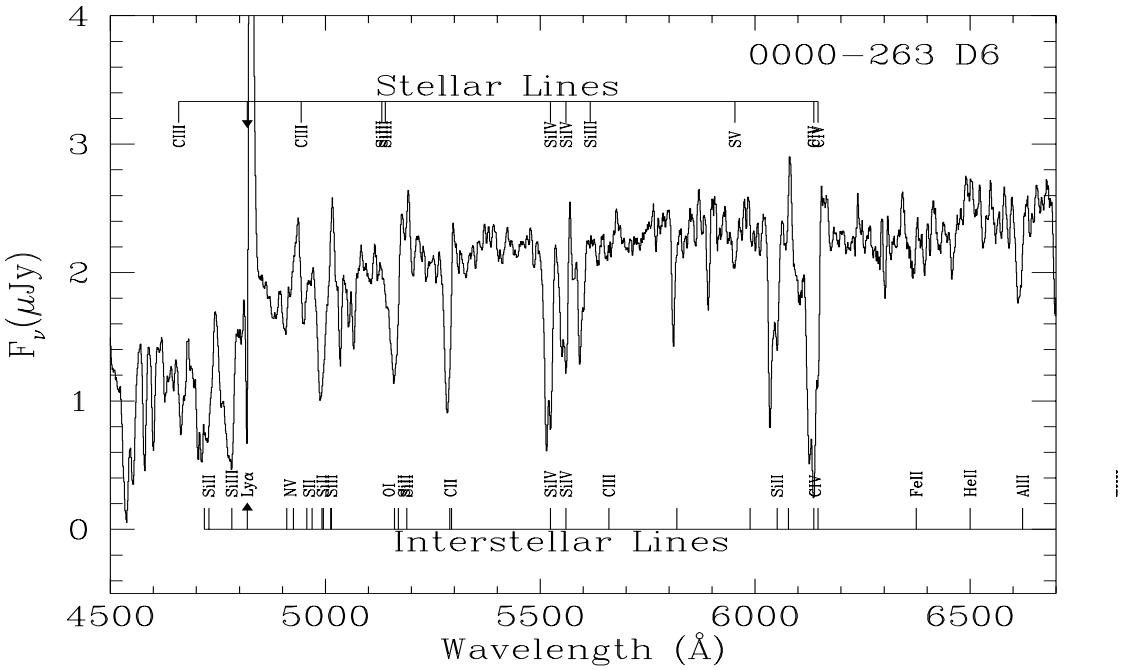

Fig. 6.— Spectra of distant galaxies at $\lambda/\Delta\lambda > 1000$ will probe stellar content, chemical abundance, and stellar and gas kinematics. This 4.8-hour $\lambda/\Delta\lambda = 1200$ spectrum of a very bright ($R \simeq 23$) star-forming galaxy at a redshift $z = 2.96$ obtained with the W. M. Keck Telescope (Dey et al. 1999) is dominated by absorption lines from the interstellar medium and stellar winds, but also shows weak photospheric absorption lines of hot stars.

surface with current studies: a typical Keck+LRIS campaign results in $\sim$ a dozen redshifts of $R \sim 24 - 25$ galaxies per night. The low-resolution spectra that are obtained probe only a restricted class of objects (mostly low-extinction, star-forming systems) and are generally only sufficient for measuring redshifts. Detailed investigations of the physical properties of these objects and their evolution requires spectroscopic capabilities which are neither available nor planned.

For the detailed spectroscopic studies described here, we need a minimum resolution of $\lambda/\Delta\lambda \approx 2000$ and signal-to-noise ratios per resolution element of ~ 20 (e.g., figure 6). The redshift range targeted by this survey requires spectroscopy at both optical and infrared wavelengths. In 0.″7 seeing with DEIMOS on Keck, this requires an exposure time of ≈ 1 night per 80-object mask; hence it will take 6250 clear nights to obtain spectra of 5×10^5 galaxies, or a minimum of 17 clear observing years with Keck and DEIMOS dedicated to this one project. In comparison, SWIFT would execute this project in only ~ 100 clear nights. A large spectroscopic study of this nature would yield a very large slit survey of 'blank' sky, resulting in a high potential for serendipitous discoveries (e.g., of extremely high redshift objects not directly targeted by the study).

2.3. Formation of the Milky Way and Its Neighbors

The study of the stars in the Milky Way (fig. 7) is a rich subject capable of revealing not only the physical structure of the Galaxy that we live in but also critical clues to its formation and evolutionary history. The current picture of galaxy formation favors the formation of large galaxies through hierarchical merging of smaller entities (fig. 8). Detailed studies of Galactic structure provide a unique context in which to test such theories and to probe the star formation and chemical enrichment history of galaxies, since in no other galaxy can we study in such detail the ages, kinematics, and metallicities of individual stars, which constitute the fossil record of galactic evolution. The Galaxy also provides a rich hunting ground for rare stellar populations of great astrophysical interest. For example, the ages of the oldest white dwarfs in the Galaxy can place stringent constraints on the age of the Universe, since the Universe must be older than the things in it.

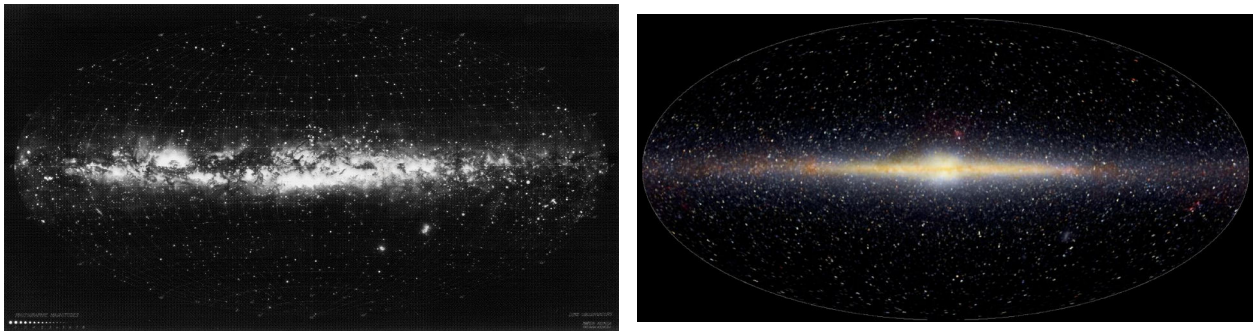

Fig. 7.— The Milky Way as seen in starlight (left; Lund Observatory) and in the infrared (right; COBE/DIRBE). The ages, kinematics and abundances of individual stars constitute the fossil record of galactic evolution.

Since many Galactic structure questions are addressed statistically, there is an intrinsic need for large samples. For example, reconstructing the formation and evolutionary history of the Galaxy relies on robust statistical correlations between stellar age, metallicity, and kinematics, as a function of position in the Galaxy, a task that depends critically on large samples. Moreover, the properties of the background stellar distribution must be determined to high statistical accuracy in order to unambiguously identify substructure arising from discrete merger or star formation events. Since the Milky Way covers the entire sky, comprehensive studies of its structure and contents (especially rare populations) intrinsically require large areal coverage. Spectroscopy is critical since it provides the only robust means of obtaining stellar spectral types, radial velocities, and metallicities. Useful stellar spectral features are available throughout the optical and infrared, the longer wavelength diagnostics being critical for studies of extincted populations.

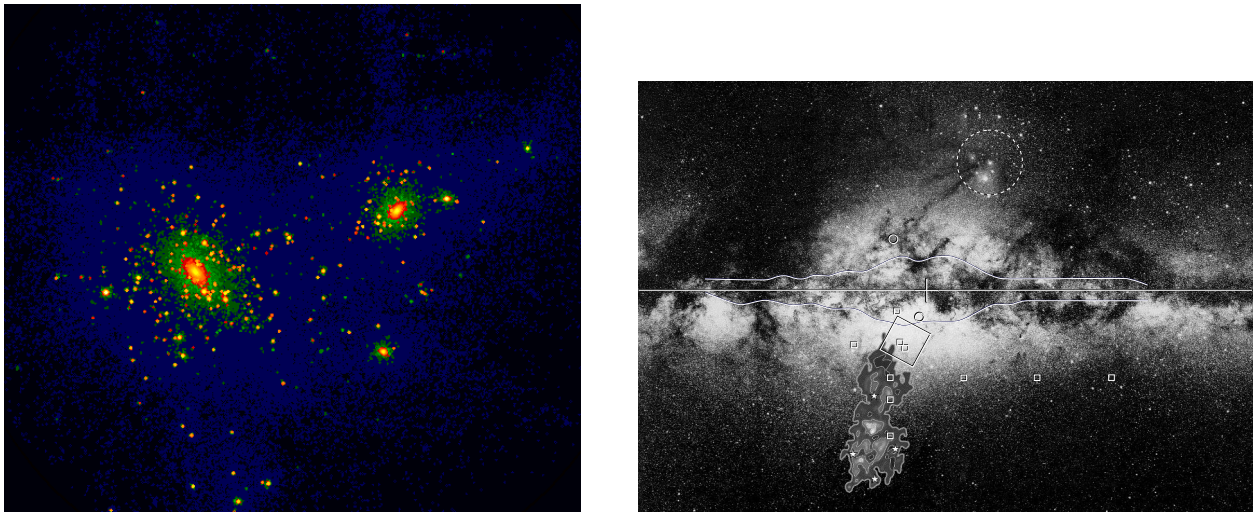

Fig. 8.— Simulations predict that large galaxies interact and merge with surrounding swarms of dwarf galaxies (*left*; Klypin 1999), while spectroscopic observations of our own galaxy have identified the remnant of one such merger in the Sgr dwarf (*right*; Ibata et al. 1994; Wyse 1997).

2.3.1. Formation of Galactic Halos

Although it contains a small fraction (∼1%) of the luminous mass of the Galaxy, the low density of the halo reduces the rate of tidal disruption and merging, allowing it to retain much of its merging history over long timescales in the form of fossil streams of stars (e.g., Tremaine 1993). Over tens of Gyr, merger remnants will spread out into tidal streamers that extend across the sky (fig. 9). The accretion of multiple satellites may result in tidal streamers covering a large fraction of the sky (>10%), with the observed covering fraction being diagnostic of the mass and total number of merged satellites. For example, if ∼100 objects of mass $\sim 10^5\,M_\odot$ were accreted by the halo in the last 10 Gyr, the resulting tidal streamers would cover 10% of the sky (Johnston 1998).

For minor mergers, the low surface density of the resulting streamers (and high background contamination) suggests that star counts alone will be insufficient to detect the streamers. Instead, the spectroscopic identification of large-scale structures with coherent kinematic motions (proper motion, radial velocity) and metallicities is required (e.g., halo moving groups—Majewski et al. 1996; discovery of the Sgr dwarf—Ibata et al. 1994). The measured kinematics and current structure of the streamer can be used to reconstruct the encounter and recover information on the Galactic potential.

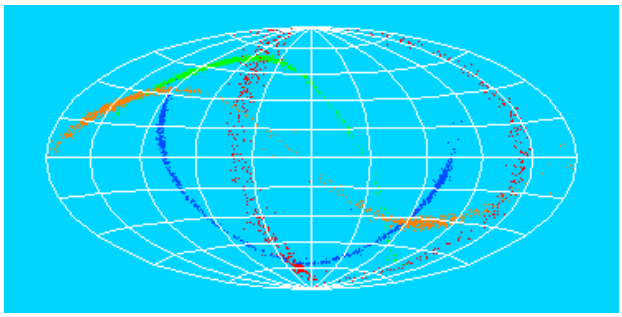

Fig. 9.— The Galactic halo may retain the memory of its merging history in the form of fossil streams of stars. Halo streamers, as depicted by Johnston et al. (1996), can be detected spectroscopically as stellar groups with coherent kinematics and metallicities.

A Representative SWIFT Project: Halo Tidal Streamers

Simulations indicate that a survey of 4000 □°(10% of sky) will reveal significant structure in the halo. Since the kinematic and metallicity properties of halo streamers may not differ drastically from the mean halo population (e.g., Majewski et al. 1996), dense sampling in each pointing (1.75□°) is needed for the robust identification of a coherent structure against statistical fluctuations in the background halo population.

At a spectroscopic magnitude limit of V=22, we will be able to detect F and G halo dwarfs to 25 kpc where we expect a few 1000 dwarfs/□° (Reid & Majewski 1993). Assuming the pessimistic case that the halo streamer population represents only a small fraction (10%) of all halo stars, we would identify ∼100 halo streamer stars per square degree. This would be sufficient to identify and quantify the mean kinematics and metallicity of the streamer population. SWIFT spectroscopy would be used to identify and eliminate interloping galaxies and to determine radial velocities and metallicities for all of the halo stars in order to search for coherent groups of stars in kinematics and metallicity.

Beyond quantifying the merger history of the halo, this project would also map out the kinematics and metallicities of ∼4 million halo dwarfs, possibly resulting in the detection of ultra metal-poor stars ([Fe/H] < -4) created in primordial star formation events. There are a host of other exciting discoveries possible in such a large dataset. Similar studies of the halos of nearby galaxies (e.g., LMC, M31, M33, M81) can be used to probe their formation histories for comparison with that of the Milky Way. Issues of interest include studies of galactic potentials, chemical enrichment histories, and existence of tidal streamers. SWIFT's field of view and high slit density are well-matched to the projected density of halo giants in these systems. Such studies may find convergent evolution occuring in galaxies with different progenitor populations. For example, the halo of M31 is thought to be much more metal rich than the Milky Way halo (e.g., Rich et al. 1996). Detailed abundances and kinematics for M31 halo giants can be used to explore the dynamical history of the halo and the origin of the high metal abundance.

2.3.2. Formation and Evolution of the Galactic Disk

Since the disk of the Milky Way comprises the bulk of the luminous mass of the Galaxy, its formation and evolutionary history provide critical clues to galaxy formation in general and to the interpretation of spatially unresolved observations of distant galaxies. Despite its significance, our knowledge of the structure of the stellar disk on size scales of tens of kpc is relatively poor due to our vantage point within the disk. As a result, disk stars can be obscured by large columns of intervening dust, and the disk subtends a dauntingly large solid angle on the sky (fig. 7). There are, nevertheless, fundamental and compelling questions about the nature, formation, and evolution of the disk that can be addressed by densely sampling the stellar kinematics and metallicities in the Galactic plane. For example, what does the stellar disk of the Milky Way look like from above? — the kinematic (e.g., spiral) structure of the disk is better traced by stars than gas since distances can be obtained for individual stars and the result is model independent. The stellar metallicity distribution in the disk contains fossil clues to both the star formation and merger history of the disk.

Simulated mergers of satellite galaxies with the Milky Way show that such encounters can produce vertical heating and thickening of the disk, as well as tilts and warps that persist for many dynamical times (> 10 Gyr; fig. 10). As the satellite is torn apart, debris is left at all disk radii as the satellite first sinks into the plane, then spirals in (e.g., Quinn et al. 1993; Walker et al. 1996; Huang & Carlberg 1997). Since the disk can be damaged extensively in fairly major mergers (satellite mass $>10\%$ of the disk mass), with the extent of the damage a strong function of the mass and density of the satellite, measurements of the structure of the Milky Way disk can constrain the role of major mergers in its evolutionary history. Measurements of the "thinness" of the thin disk, when combined with the ages of the oldest objects in the thin disk, can be used to determine the time since the last major merger.

A Representative Project: Galactic Plane Survey of K-giants

Clues to the Milky Way's merging history can be obtained from searches for (1) merger remnants that have spiraled in to the disk, and counter-rotating streams from retrograde mergers (isolated through kinematics and chemical abundances), (2) tilts and warps, and (3) the radial variation of the vertical velocity dispersion. K giants are excellent tracers of disk structure since they can be seen across the entire Galaxy, are not restricted to young stellar populations, and are abundant enough that studies of large samples are possible. Along a given line-of-sight that probes the entire Galaxy ($\gtrsim$20 kpc in depth), we require a sample of $>$1000 stars in order to achieve a spatial resolution of $\lesssim$1 kpc with $\gtrsim$100 stars in each radial bin in order to characterize the mean and spread in metallicity, the stellar

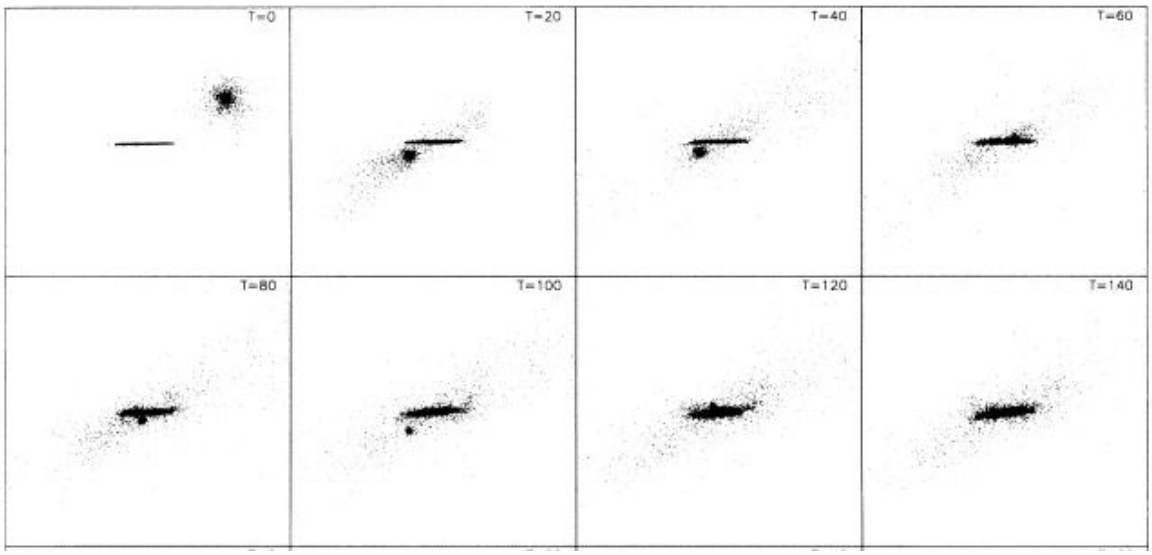

Fig. 10.— Simulated mergers of satellites with disk galaxies produce long-lived tilts and warps, vertical thickening of the disk, and merger debris scattered throughout the disk (Huang & Carlberg 1997). Since stars maintain the fossil record of galactic evolution, densely sampled spectroscopic study of the kinematics and metallicities of disk stars can recover the merger and star formation history of the Galaxy.

kinematics, and any relation between the two to a few percent. K giants have the requisite density: at $\ell = 35$, $b = 0$, the K giant density is $\sim 10^4/\square^\circ$, decreasing to $\sim 1000/\square^\circ$ at $b \sim 6$. A survey of the inner Galaxy ($\ell = 35 - 75^\circ$, $b = \pm 5^\circ$) would yield a sample of $\gtrsim$400,000 stars.

K giants (to $I \approx 22$, assuming a maximum $A_V \approx 12.5$) can be identified (using, e.g., the CO index) and proper motions measured from near-IR wide-field imaging surveys. Radial velocities, metallicities (from Ca triplet), and line-of-sight gas column densities would be measured with SWIFT at a spectral resolution of $R \simeq 5000$. The entire spectroscopic program can be completed in ~ 225 clear nights. The comparison with the observing time required with other observing systems is shown in table 1.

Beyond providing valuable constraints on the merger history of the disk, the potential results and legacy of such a study would also include: (1) Chemical evolution of the Galactic plane, as extracted from the metallicity distribution for different kinematic populations as a function of position in the Galaxy. (2) Mass distribution of the Galaxy, as constrained by the phase space distribution of 400,000 stellar test particles. (3) A map of extinction and gas/dust ratio along 400,000 lines of sight through the Galaxy.

2.3.3. Age of the Disk and Halo

The remnants of the earliest star formation events in the Galaxy are currently observable as the coolest white dwarfs. Since the cooling rate of white dwarfs is fairly well-known (e.g., Saumon & Jacobson 1999, Hansen 1999), they can be age-dated based on their observed luminosities. The luminosity function for white dwarfs has consequently been argued as a robust and independent measure of the age of the Galaxy and its star formation history (e.g., Winget et al 1987, Leggett et al. 1998).

The extreme faintness of the oldest white dwarfs ($M_V \gtrsim 16$; fig. 11) restricts the volume in which they will be detected to the solar neighborhood. While recent work has led to preliminary determinations of the age of the Galactic disk by this method (e.g., Leggett et al. 1998) larger area and deeper searches would firmly establish the age of the disk as well as enable the first studies of halo white dwarfs. Ages for the rare halo white dwarfs ($\sim$ 3–10% of disk white dwarfs by number) would place unique constraints on the age of the halo and consequently the age of the Universe.

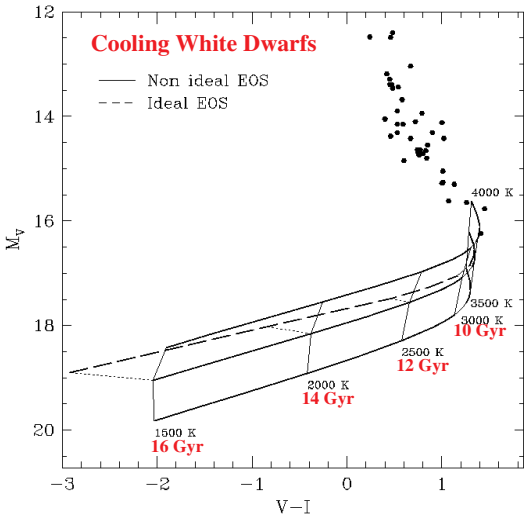

Fig. 11.— Because their cooling rates are well-understood, cool white dwarfs ($M_V > 17$) offer a robust and independent measure of the age of the Galaxy and a constraint on the age of the Universe (e.g., Saumon & Jacobson 1999). Spectroscopy is required for detection since significant contamination remains even after photometric selection criteria have been applied.

Since both low metallicity stars and distant galaxies have colors similar to those of cool white dwarfs, the detection of cool white dwarfs requires spectroscopy because of the significant contamination that remains even after photometric selection criteria have been applied (fig. 12). New photometric selection techniques (Claver 1995) are currently able to weed out many of the potential contaminants, leaving roughly 10 contaminants for every bona fide white dwarf. Of these, only a small fraction have the low luminosities ($M_V > 17$; $L/\,L_\odot < -4.5$) that are capable of determining the ages of the disk and halo.

A Representative Project: Cool White Dwarfs in the Halo and Disk

A magnitude limited spectroscopic survey provides a kinematically unbiased method for

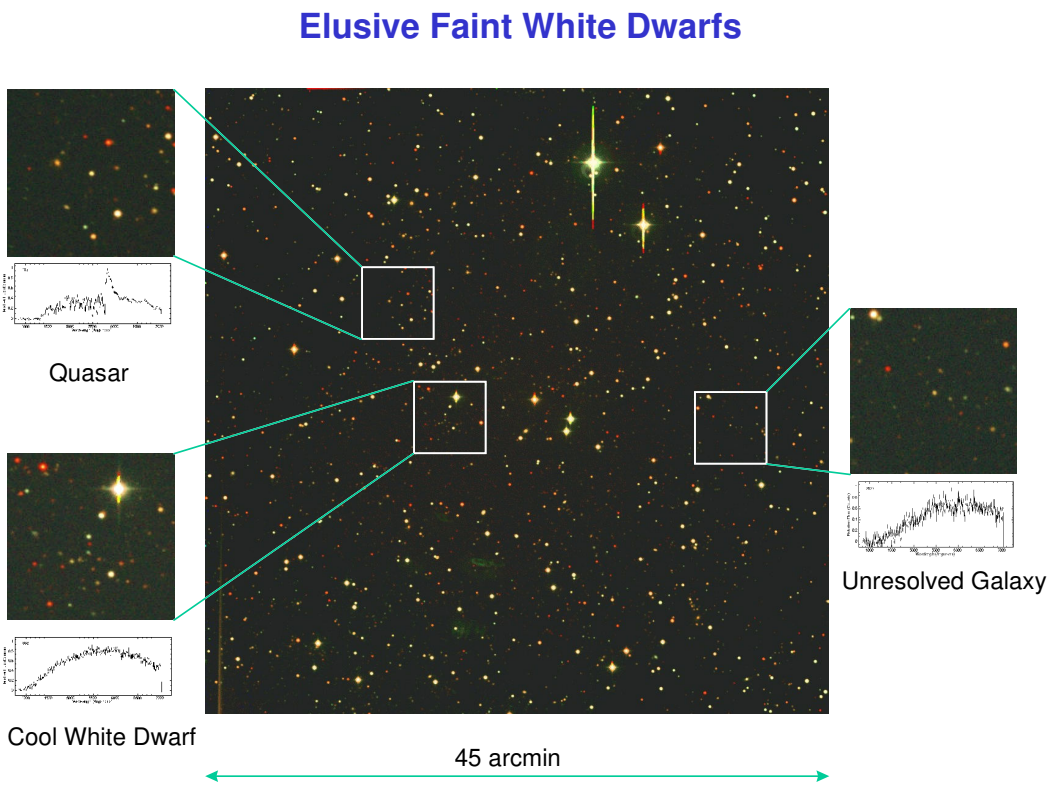

Fig. 12.— Searching for a needle-in-a-haystack. In this shallow 45' field, photometric selection criteria identify ∼30 white dwarf candidates to V=18.5. Follow-up spectroscopy revealed that, of these, 3 are bona fide white dwarfs, but all are 4–5 Gyr old, much younger than of interest. Deep spectroscopy over a wider field of view is needed to detect old disk white dwarfs and the even rarer halo white dwarfs.

culling out the coolest white dwarfs in the solar neighborhood. Results from this survey will be critical toward quantifying the kinematic selection biases of future large-area ($\sim 10,000\square^\circ$) proper motion surveys of the halo white dwarf population. A reasonable compromise in survey area and depth is a survey for white dwarfs over $100\square^\circ$ to a limit of V=25 in order to probe white dwarfs with ages $>$ 10Gyr. At this magnitude limit, photometric selection will whittle down the number of white dwarf candidates to a manageable $\sim 2000/\square^\circ$. Of these, ∼200 will be bona fide white dwarfs and ∼1 will be in the critical range $\log(L/\mathrm{L}_\odot) < -4.5$. Currently known disk white dwarfs in this luminosity range number between 1 and 5. Therefore, in establishing accurate statistics at $\log(L/\mathrm{L}_\odot) < -4.5$, a survey of $100\square^\circ$ will definitively establish the age of the disk. Of the ∼100 cool white dwarfs that will be detected in the survey, 3–10% will belong to the halo population, enabling an initial estimate for the age of the halo. The survey will thereby provide a self-consistent estimate for the relative ages of the disk and halo, both of which have been obtained from the same method and models.

3. SYNERGY WITH GROUND-BASED IMAGING SURVEYS

The Explosion in Wide-Field Imaging: The last 5 years have witnessed a dramatic increase in wide-field imaging capabilities on moderate and large aperture ground-based telescopes (Table 2). The KPNO and CTIO 4-m telescopes, the CFHT, Subaru and the upgraded MMT all boast optical imaging cameras with fields of view $\approx 30'$, and have prompted a host of wide-field survey projects that drive an immediate need for deep wide-field spectroscopy of extremely large samples. The wide-field surveys ongoing or completed at the time of writing are summarized in Table 3.

Table 2: Existing & Planned Optical Wide-Field Imaging Cameras

Telescope	Aperture (m)	Camera	FOV (′)	Years of Operation	# Sq. Deg by 2010[1]
Mayall	3.8	MOSAIC	$36' \times 36'$	1998-2010	1,240
KPNO 0.9m	0.9	MOSAIC	$59' \times 59'$	1998-2010	220
Blanco	3.9	BTC	$4 \times 15' \times 15'$	1997-1999	250
Blanco	3.9	MOSAIC	$35' \times 35'$	2000-2010	1,050
CFHT	3.6	UH8K	$29' \times 29'$	1998-2000	200
CFHT	3.6	CFHT12K	$42' \times 28'$	2001-2005	480
CFHT	3.6	Megacam	1 sq. deg.	2001-2010	2,700
Hale	5.0	LFC	$23' \times 23'$	2001-2010	720
Subaru	8.3	SUPRIME-CAM	$34' \times 27'$	2000-2010	3,960
MPG/ESO	2.2	WFI	$34' \times 33'$	1999-2010	1,000
VST	2.5	ΩCAM	$60' \times 60'$	2005-2010	2,300
VISTA	4.0	Optical	$96' \times 84'$	2005-2010	12,600
Magellan	6.5	IMACS	$27' \times 27'$	2005-2010	1050
MMT	6.5	Megacam	$24' \times 24'$	2005-2010	700
3DT 8.4m	6.9		$180'$ dia.	2007-2010	2x42,000

[1] Equivalent area covered to R=26 AB (5σ, 2" aperture) in a single filter assuming 20% of time is utilized for imaging. In the case of the VLT Survey, VISTA and 3DT 8.4m imaging telescopes, it was assumed that only 60% of the time was used for imaging. The benchmark used was that the Mayall + MOSAIC reaches this depth per field in 2 hours (including overheads), and therefore covers roughly 1.4□° per clear night.

As an example, the NOAO Deep Wide Field Survey is obtaining images in B_W, R, I, and K of two 9□° patches to a depth of 26 AB mag in the optical bands. The source catalogues generated by this survey are of the order of $\sim 10^5 - 10^6/\square^\circ$. For subsets of objects, the source densities remain high: $z \gtrsim 3$ galaxies, for instance, are $\gtrsim 4,000/\square^\circ$, and emission line galaxies selected from complementary narrow-band imaging surveys in

Table 3: Ongoing Optical and Near-Infrared Surveys

Survey	O/IR	$M_{\rm AB}^{\rm limit}$ mag.	Area sq. deg.	Completion Date
2MASS	IR	15	42,000	
SDSS	O	23	10,000	
MACHO	O			
LCO/UCO	O	22	130	
CFHT-RZ	O	25	50	
BTC40	O	25	40	
NOAO-opt	O	26	18	2001
NOAO-IR	IR	21	18	2001
Hawaii	O	25	>15	
EIS-Wide	O	23	17	
Deeprange	O	23	16	1997
CNOC2+	O	24	6	2001
BFQS	O	25	7	1998
CNOC2	O	24	1.5	
CFDF	O	25	1	
CFHT-VRZ	O	26	1	

these fields have source densities to $\sim 1500/\Box^\circ$ (for sources with line fluxes brighter than 3×10^{-17} erg/s/cm^2).

The Need for Highly Multiplexed MOS Spectroscopy: Reaping the science benefits from these surveys requires a vast amount of spectroscopic follow-up. Although a few of the surveys are imaging-only programs (e.g., the weak lensing surveys), the majority of the surveys currently underway are designed to pre-select certain types of objects for detailed spectroscopic study. The surveys designed to investigate galaxy formation and evolution, the evolution of large-scale structure, cosmology (e.g., using SNe), Galactic structure, cluster searches, high-redshift ellipticals, the red-envelope galaxy population, radio sources, etc., all fall into this category. Imaging alone may indeed be adequate for a few projects. However, in order to understand the astrophysical processes, spectroscopy is essential. In general, the imaging surveys are only the first step: spectroscopic follow-up is critical.

The current suite of spectrographs available at large-aperture telescopes will barely begin to meet the need generated by the current imaging surveys. This is clearly evident from the fact that time requests for spectroscopic follow-up of imaging surveys from HST

and various 4-m and 5-m telescopes alone exceed the time available on the Keck Telescopes. Moreover, a typical LRIS + Keck night results in low resolution spectra of about 15-30 objects with $R \approx 24.5$ at a signal-to-noise ratio too poor to yield much other than basic redshift information. To go beyond this and study the internal dynamics, chemical composition, stellar content, age, and mass of the galaxies requires a significantly larger investment of observing time. Although the existing large-aperture telescopes will provide pathfinder science by spectroscopically observing manageably small, carefully selected samples from the imaging surveys, they will not be able to carry out spectroscopy on the scale that is required for a comprehensive understanding of the astrophysics.

Finally, the most interesting discoveries are sometimes serendipitous (e.g., the first galaxy at $z > 5$); spectroscopy maximizes the discovery potential of a survey.

Synergy with Ground-based Radio/Sub-mm Observations:

A highly multiplexed spectroscopic capability provides a necessary complement to ground-based radio initiatives. For example, by virtue of the negative K-correction at millimeter wavelengths for distant dusty galaxies, future deep Millimeter Array (MMA) surveys have the potential to detect very high redshift sources ($z \sim 5 - 10$). The existence of an abundant dusty star-forming galaxy population is supported by recent deep surveys at sub-millimeter wavelengths (e.g., Smail et al. 1997). For the faint sources detected in deep pointings with the MMA, optical and near-infrared spectroscopy will be essential in order to determine their redshifts and relationship to known star-forming galaxies at high redshift. The source densities of these objects is likely to be very high: a typical 1 hour observation with the MMA will identify sources to $\sim 100\mu$Jy at 850μm ($> 10\sigma$); the source densities to these flux densities are unknown, but current predictions (e.g., Franceschini et al. 1998) suggest $> 50,000/\Box^{\circ}$!

4. SYNERGY WITH SPACE-BASED MISSIONS

The New Character of Ground-Based Support for NASA Missions: By 2010, a host of NASA missions will be generating images of the sky at wavelengths from γ-Rays to the far-infrared. Some of these missions will provide all-sky surveys whereas others will provide deep images of small (1-100$\Box^\circ$ sized) regions of the sky. The much greater sensitivity of these NASA missions (Chandra/AXAF, SIRTF, GALEX, FIRST, Constellation-X) compared to previous missions is expected to produce detections of typically 1000 - 10,000 objects/$\Box^\circ$, orders of magnitude higher than previous missions (please see Table 4). The new character of NASA missions calls for much more efficient modes of spectroscopic followup, i.e., the highly multiplexed multi-object spectroscopy of SWIFT.

Table 4: Source Densities for Present and Future NASA Missions

Mission (Launch)	λ	FOV ($'$)	$t_{\rm exp}$ (sec)	$F_{\rm lim}$/band	$N_{\rm sources}$ per sq.deg.	Surveyed Area (deg^2)
SIRTF	MIR/FIR	5	12	88μJy/3.6μm	2000	
(2001)			5×200	4μJy/3.6μm	72000	
NGSS	MIR	34		$\sim 100\mu$Jy/3.6μm	~ 2000	42000
(2004)						
GALEX	UV	75	100	21.7AB/(0.13-0.3μm)	260	42000
(2003?)			20000	26AB/(0.13-0.3μm)	6500	200
ROSAT	X-ray					42000
(1990)				10^{-18}W/m^2/(0.5-2keV)	970	0.3
Chandra	X-ray	17-30	typical	10^{-17}W/m^2/(0.2-10keV)	300	500
(1999)			deep	10^{-19}W/m^2/(0.2-10keV)	2000-10000	50
XMM	X-ray	30	10–	10^{-17} –	300–	100-200
(2000)			100 ksec	10^{-18}W/m^2/(0.1-4.5keV)	–1000	(GTO)

These missions will require both ground-based optical and near-IR imaging (to identify the optical and near-IR counterparts of the objects detected in the space-based surveys) as well as optical and near-IR spectroscopy (in order to classify the object, determine its redshift, and understand its physical properties - composition, internal dynamics, bulk motion, kinematics, stellar content, formation history, mass, age, etc.).

Spectroscopic Follow-up of Many Faint Sources per Square Degree: Typical source densities for objects detected by these surveys is of the order of $3 \times 10^2 - 10^5/\Box^\circ$ (Table 4). The optical and near-infrared counterparts of the bulk of the sources detected by the NASA

missions will range between 19-27 AB mag.

For example, at X-ray wavelengths, typical Chandra images to $F_X(2-10\ \mathrm{keV}) = 10^{-14}$ erg/s/cm^2 will contain about 300 sources/$\Box^\circ$. The deepest Chandra pointings (to $F_X(2-10\ \mathrm{keV}) = 3\times10^{-16}$ erg/s/cm^2) will contain about 2,000-10,000 sources/$\Box^\circ$ — completely uncharted territory! Although ROSAT succeeded in resolving part of the X-Ray background, the nature of the objects responsible for the soft-X-Ray background, i.e., whether they are normal galaxies or a new population of low-luminosity or obscured AGN, remains a mystery. Understanding the nature of this faint population, and their relationship to normal galaxies, will require spectroscopy of a significant fraction of these high surface-density sources.

The source density limits are comparable at mid-/far-infrared wavelengths: deep SIRTF exposures (5×200 seconds with IRAC) will reach 4μJy at 3.6μm, and should have source densities of about 72,000 sources/$\Box^\circ$. More typical exposures of 12 sec will reach 88μJy and have field source densities of 2,000 sources/$\Box^\circ$. The SIRTF surveys will uncover dusty galaxies at intermediate and high redshifts, and possibly identify sources which are missing from our optical catalogs due to their red colors. The dusty galaxy population may contribute significantly to the global star formation and metal production rate at early epochs, and little is known about this population at present. Similarly, GALEX, which operates at UV wavelengths, will obtain near- and far-UV imaging surveys in fields of 200$\Box^\circ$ to 26 AB mag and over the entire sky down to 21.7 AB mag, with typical source densities (for extragalactic objects) at these two limits of 6500 and 260/$\Box^\circ$ respectively.

Even at optical and near-infrared wavelengths, space-based facilities have resulted in a vast quantity of exquisite imaging data. *Hubble Space Telescope* imaging programs (using the WFPC2 and NICMOS cameras) have resulted in exciting discoveries, but many of these projects have been critically reliant on spectroscopic observations obtained with ground-based telescopes.

Comprehensive Follow-up Maximizes Scientific Return: It is imperative to have spectroscopic observations of very large numbers of the detected sources in order to maximize the scientific return from the NASA space missions. The reasons are twofold: first, the most interesting scientific return is usually in identifying the various populations that are detected at other wavelengths (i.e., X-Rays, UV, IR, Sub-mm), quantifying their contribution to the total source population and understanding their cosmological significance. At the faint end, where the source densities are high and follow-up requires a highly multiplexed capability, the resolved sources may contribute significantly to the extragalactic background and are of importance to cosmology and galaxy evolution. Second, the most unusual source, and one which often provides a critical astrophysical clue, is

invariably hidden in the vast number of sources at the catalog limit. For example, IRAS FSC10214+4724, the most luminous infrared source in the Universe, was only barely detected by IRAS and found only by spectroscopically surveying a very large sample of faint IRAS sources. The potential for serendipity is enormous with a large-scale ground-based spectroscopic effort complementing the planned space missions.

5. TECHNICAL FEASIBILITY OF SWIFT

The guiding design principle of SWIFT is that it is an integrated telescope+spectrograph optimized for wide-field, extremely efficient, and highly multiplexed slitlet spectroscopy. To achieve this goal, the spectrograph and telescope optics are designed together as a system. The primary design objective is to preserve as wide a field of view as possible on as large an aperture as possible without compromising the capability for highly efficient beam-fed spectroscopy. In this section, we outline one possible realization of SWIFT which minimizes risk and can be built at the present time. Although the current design demonstrates the technological feasibility of the concept as an 'existence theorem', in practice there are various technological paths we intend to investigate in order to maximize the scientific effectiveness of this facility and enable us to determine the relevant technological paths to future instrumentation on the next generation of large-aperture telescopes.

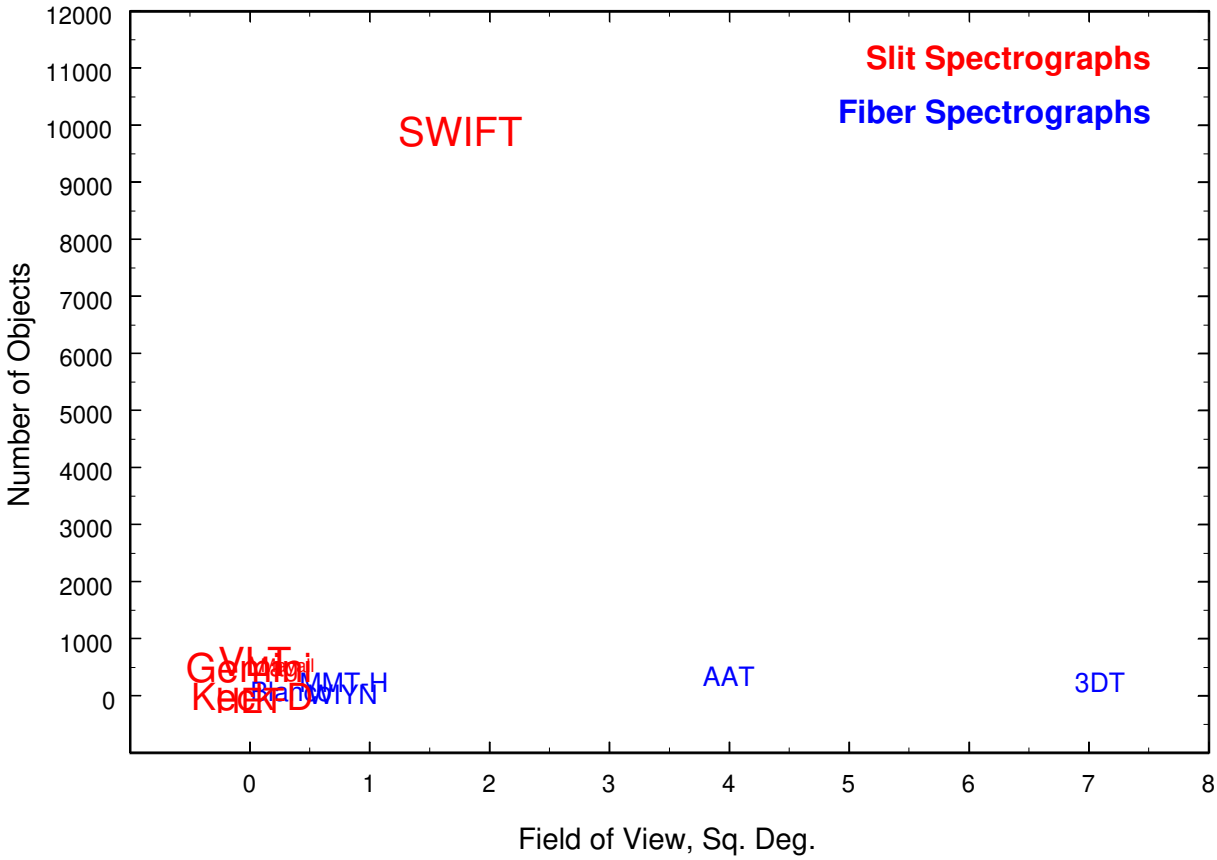

Fig. 13.— SWIFT occupies a unique region of parameter space when compared with existing and planned multi-object spectrographs. Fiber systems are shown in blue, beam-fed systems in red. The size of the labels is proportional to the limiting magnitude. SWIFT can target 2000–10000 sources at a time.

Table 5: Baseline Concept for SWIFT

Fore-optic	>8-m diameter effective aperture
Field of view	1.5° diameter
Wavelength range	0.36 — 1.7μm
Spectral resolution	500, 5000, 25000
Image quality	<0.″25[1]
Slitlet density	2000—10000
Total system throughput	∼50% optical; ∼40% near-IR
Detectors	4×16K $\times$ 16K CCD Mosaics
	4×8K $\times$ 8K InSb Mosaics

[1] 80% encircled energy diameters for 'white' light (0.36—1.7μm) over the entire field.

Table 6: Existing & Planned Spectrographs on Large Aperture Telescopes

Telescope	Aperture	Spectrograph	η[1]	FOV	N_{max}(obj)[2]	Comments
WIYN	3.5	Hydra	0.05	60′ dia.	100	fiber
Mayall	3.8	SamSpec	0.45	$40' \times 30'$		slit
Blanco	3.9	Hydra-CT	0.05	40′ dia	138	fiber
AAT	3.9	2DF	0.05		400	fiber
Magellan	6.5	IMACS	0.3?	$27' \times 27'$	600	slit
MMT	6.5	Hectospec	0.24[3]	60′ dia	300	fiber
MMT	6.5	Binospec	0.40	$2 \times 8' \times 15'$	< 150	slit
3DT 8.4m	6.9		0.1?	180′ dia.	< 500	fiber
Gemini	8.1	GMOS	0.40	$5.5' \times 5.5'$	<600	slit
VLT	8.2	VIRMOS	0.3?	$4 \times 7' \times 7'$	150-750	slit
Subaru	8.3	FOCAS				slit?
HET	9.2	LRS	0.40	4′ dia.	13	slit
Keck	10	LRIS	0.35	$5' \times 7'$	20	slit
Keck	10	DEIMOS	0.35	$16' \times 5'$	80	slit
GTC	10	ODIN	0.05?	12′ dia	60	fiber
GTC	10	OSIRIS	?	8′ dia	15	slit
GTC	10	EMIR	?	6′ dia	∼10	fiber or slit?
SWIFT	8.4		0.45	90′ dia.	2000-10000	slit

[1] Optical throughput of spectrograph and telescope.

[2] Maximum number of objects which can be simultaneously observed.

[3] Sky subtraction with fibers sets a limit of $R \sim 21$ mag on faint-object spectroscopy.

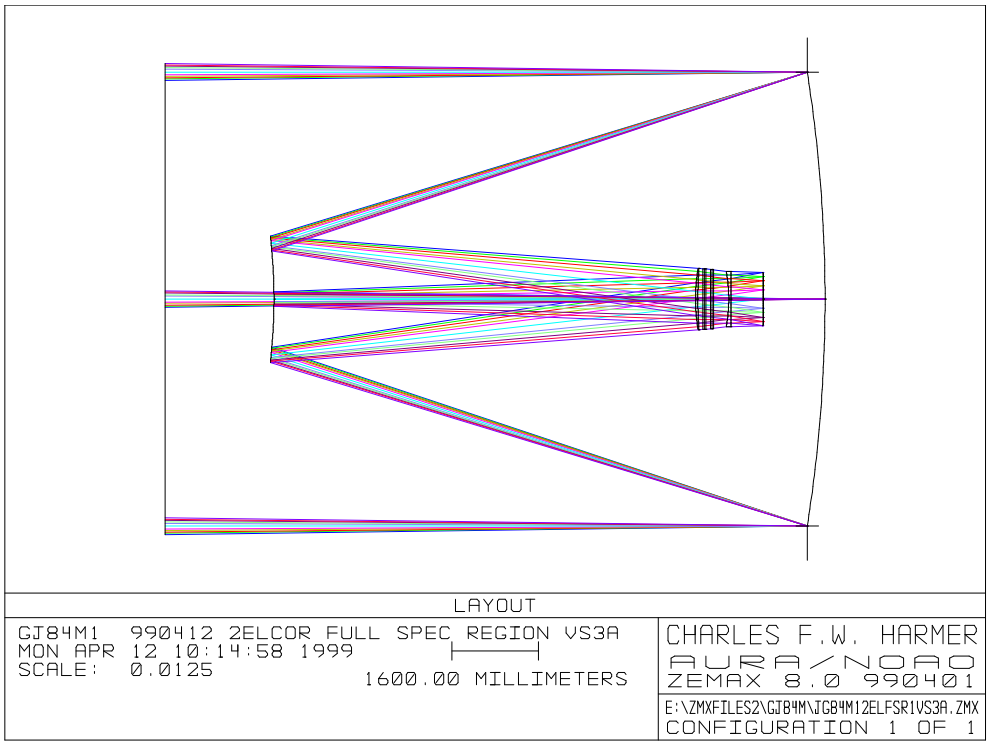

Fig. 14.— The ray trace diagram for the SWIFT telescope optics. The focal surface is in front of the primary and is curved with a maximum excursion of 7 mm from field center to edge.

5.1. The Front-End Optics: Telescope + Corrector

The fore-optics design builds on proven technology by adopting a hybrid Ritchey-Chretien system to achieve excellent image quality over as wide a field as possible. The choice of this simple design also minimizes construction delays for the telescope, which is traditionally a long lead-time item. Our baseline concept assumes an 8.4-m f/1.6 hyperbolic primary and a 2.4-m secondary ($\approx 8\%$ central obscuration) which produce a f/4.3 beam (plate scale of 5.3″/mm) at a forward Cassegrain focus. We will be investigating faster focal ratios that may reduce the overall cost of the telescope, but the present combination produces a field which can be corrected by currently buildable (and affordable!) optics. The reflecting surfaces will be coated with a protected silver coating in order to maximize the reflectivity over the 0.36–1.7μm wavelength range.

The curved field delivered at the secondary focus is corrected using a two-element aspheric fused silica corrector, each roughly 1-m in diameter (Figure 15). This results in

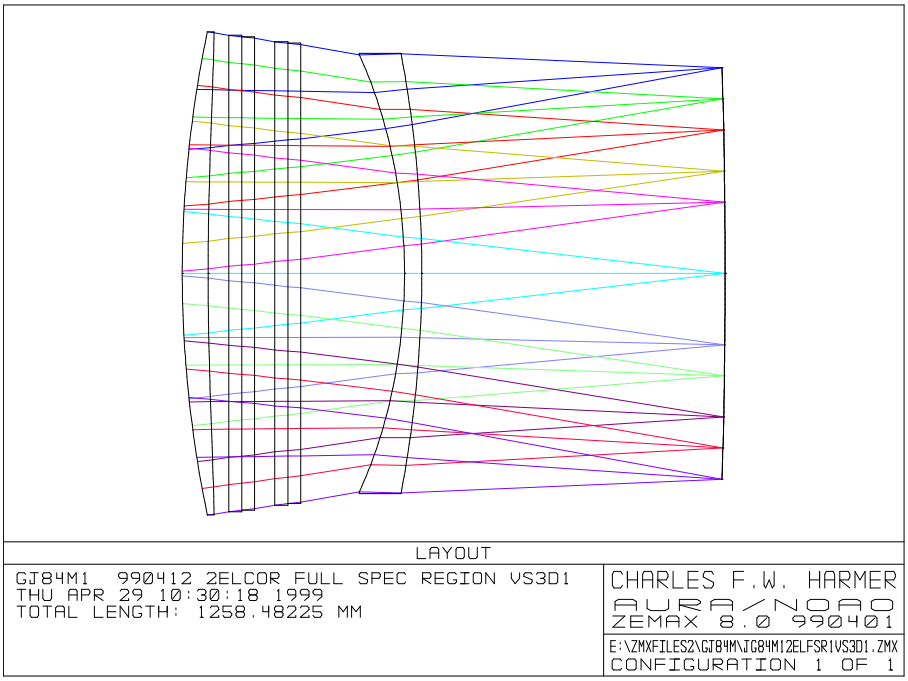

Fig. 15.— Preliminary design of the wide–field corrector for SWIFT. The corrector has two fused silica aspherics. The atmospheric dispersion compensator (ADC) is denoted notionally as two pieces of plane LLF6 glass and two pieces of fused silica.

a corrected 1.5° diameter circular field with excellent image quality (figure 16): the 80% encircled energy diameters for white light (i.e., 0.36-1.7μm) are less than 0.25″ over the entire 1.5° field! For a typical observation spanning an octave in wavelength, the 80% image diameter is $< 0.2''$. In order to compensate for atmospheric dispersion, an ADC assembly is inserted between the elements of the corrector assembly (Figure 15). The ADC is constructed from fused silica and LLF6 glasses. The latter introduce a roll-off in the transmission below 3600Å; we are investigating alternate designs that do not require LLF6, but the present design works well and meets the science requirements. The elements of the corrector and ADC are roughly 1-m in diameter. Obtaining good quality glass of this size is possible, but may require a special run at Schott. This difficulty is reflected in the cost estimate for the corrector.

5.2. The Spectrograph Optics

Since a monolithic spectrograph poses several technological challenges, our baseline concept subdivides the focal surface into 4 equal quadrants, each having a diameter of

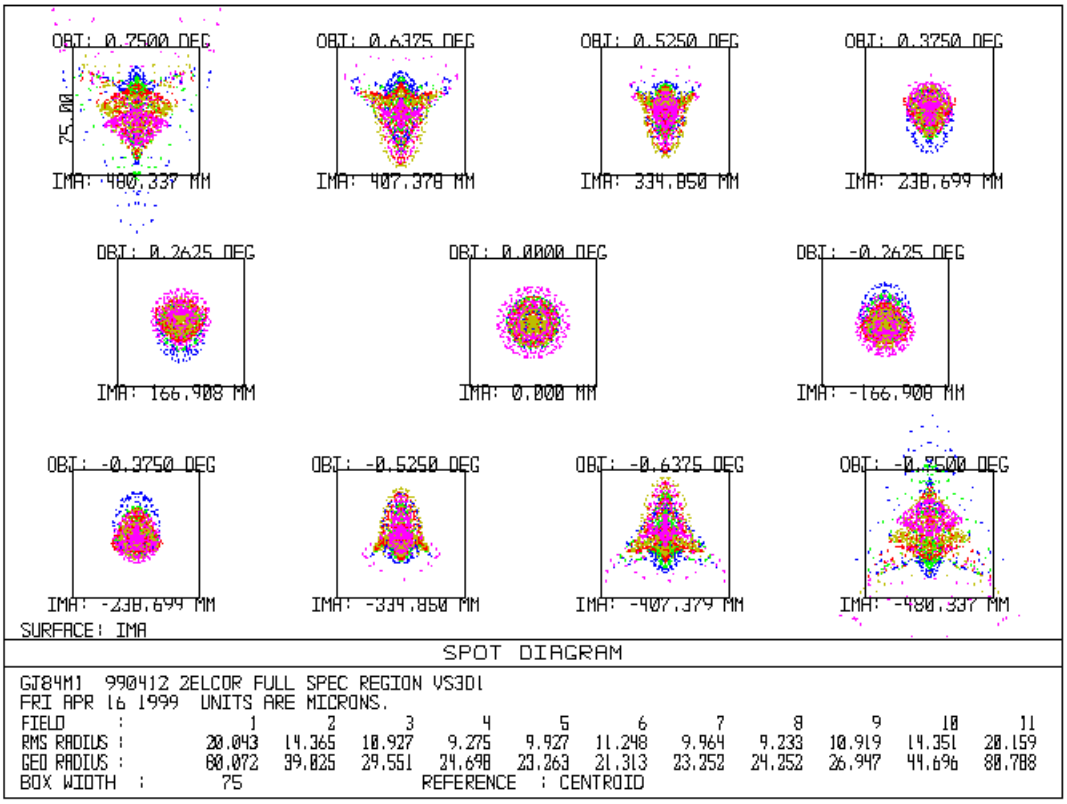

Fig. 16.— Spot diagrams are shown for SWIFT across the field of view. Each box is 0.42″ on a side. The worst images at the edge of the field, over the full spectral range 0.36 to 1.7 μm, have 0.25″ diameters.

$\approx$0.7° on the sky, and each feeding a separate spectrograph. This modular spectrograph approach offers a lower cost and lower risk to building large spectrographs, thus providing a possible design pathway for even larger instruments on future telescopes such as MaxAT. Even with this modular approach, the optical components of the design are large—the collimator optics and grating are roughly 0.4-m in diameter. Figure 17 shows the collimator design for two of the four spectrograph channels. The design of one of the f/2.4 cameras is shown in Figure 18.

The anti-reflection coatings on the lenses will probably be SolGel/MgF_2. With these coatings it is possible to keep reflection losses below 1.5% per surface over the entire spectral region (0.36–1.7μm).

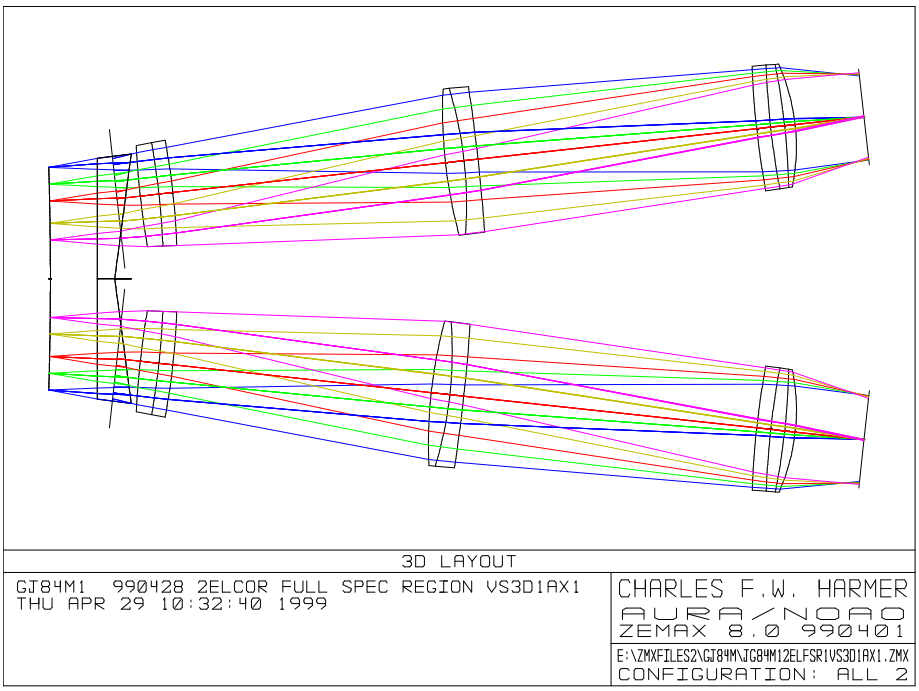

Fig. 17.— The ray trace diagram for the SWIFT spectrograph, showing the collimator design for two arms of the spectrograph. In this preliminary design, where the focal surface is subdivided into four 0.7° circular adjacent fields, the apex of the field is unused. We are currently investigating alternate designs which maximize the field usage.

5.3. New High-Efficiency Grating Technology

A relatively new grating technology promises significant advances in the performance of the next generation of optical and near-IR astronomical spectrographs. Volume-phase holographic (VPH) gratings diffract light by refractive index modulations within a thin layer of material sandwiched between two glass substrates. VPH gratings can achieve higher diffractive efficiencies in many applications than currently available surface gratings, and offer improved longevity since the grating volume is actually encapsulated between two substrates.

NOAO has been developing the technology to design and build VPH gratings in collaboration with Kaiser Optical Systems Inc. These gratings have transmission efficiencies $\gtrsim 90\%$; the highest efficiency grating tested to date has a transmission of $\approx 93\%$. Figure 19 shows the predicted total system throughput for the telescope and spectrograph (ignoring slit losses) for the baseline concept described here and for the specific case of resolution R=5000. The model for the grating efficiency has been verified using actual laboratory measurements of VPH gratings. The improvement in efficiency over Keck+LRIS comes

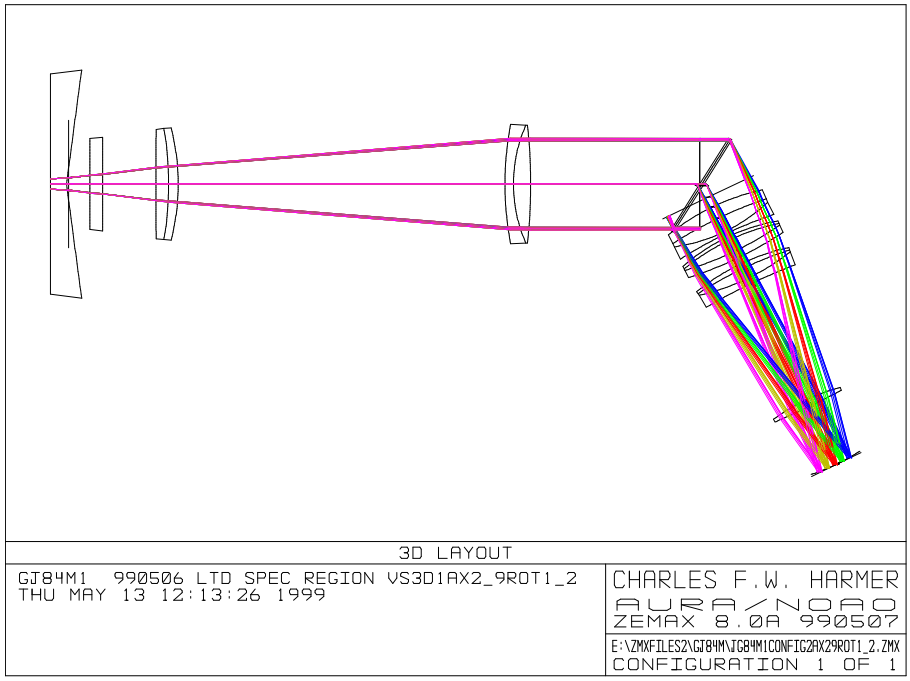

Fig. 18.— The ray trace diagram for the SWIFT spectrograph camera. In the present design, the camera must be angled away from the grating for optimum efficiency. Having four separate camera modules offers a way to balance the spectrograph load azimuthally.

partly from the use of the higher efficiency grating, but also partly from the use of protected silver coatings (similar to that being developed for Gemini North) on the primary and secondary surfaces.

5.4. Slitlet Density with SWIFT

In a low resolution (R=500) mode with a wavelength coverage of 4000Å, the slits can be separated by $5'$ in the spectral direction. Assuming $8''$ slitlets, and no space between slitlets in the spatial direction, each arm of the spectrograph can observe about 2200 targets, and each SWIFT observation results in about 9,000 non-overlapping spectra. At very high resolutions (R>10,000) targetting specific spectral regions, observations can be prefiltered through a narrower bandpass ($\Delta\lambda < 150$Å) and even larger numbers of slits ($> 10,000$) can be used. In a mode requiring spectral observations at R=5000 covering about 2000Å, the slits can be separated by about $30'$, resulting in ≈2,000 slits over the entire 1.5° field.

Innovations using 'microslits', tiny apertures $\sim 1''$ in size, used in conjuction with telescope nodding and simultaneous charge-shuffling, can permit an increase in the slit density by a factor of 10, allowing simultaneous spectroscopy of nearly 10^5 targets! Recent

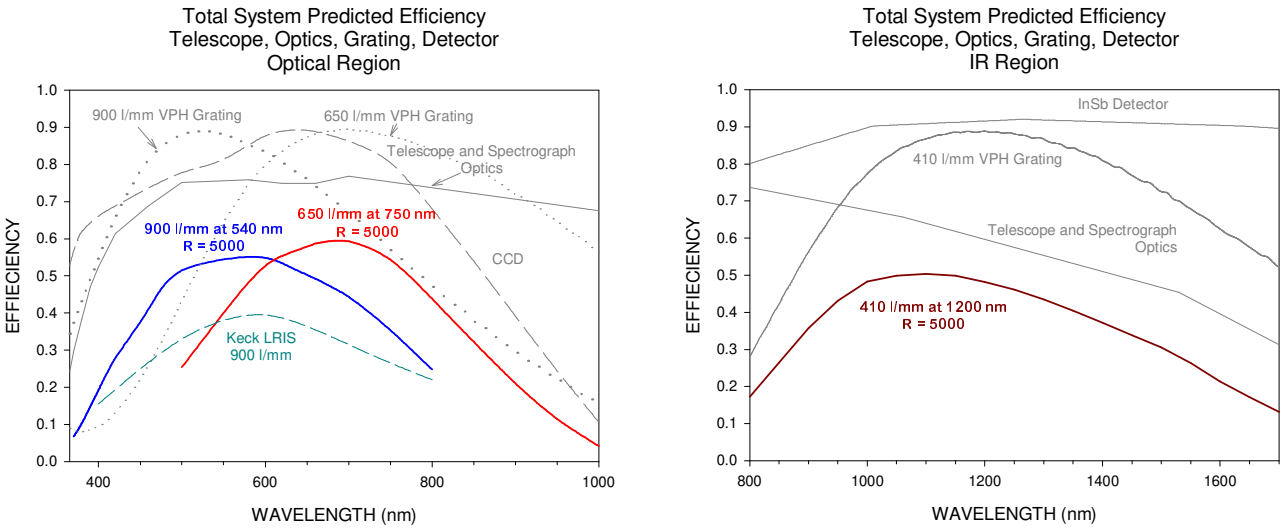

Fig. 19.— The anticipated total system efficiency for SWIFT, exclusive of the atmosphere and the slit losses, exceeds 50% across the optical (Left) and 40% across the near IR (Right). The CCD characteristics adopted are those of typical SITe 2Kx4K CCDs, such as those used in the NOAO Mosaic camera. The IR efficiency is lower relative to the optical efficiency because the optical coatings (simple SolGel/MgF_2) were optimized for 5000 Å in the scenarios represented here.

experiments with this technique at the Anglo-Australian Telescope have been successful, and these methods show great promise (see AAO Newsletter of November 1998). We will also explore slitless spectroscopic modes of operation.

5.5. Detector Requirements

While the optimal detectors for the baseline concept require 25–40μm pixels, most CCDs available today have 15$\,\mu$m pixels. Therefore, in order to image the full focal surface and provide a sufficient number of spectral resolution elements, we plan to use a mosaic array of 32 2Kx4K SITe (or equivalent) 15$\,\mu$m CCDs per spectrograph channel to yield an equivalent array of 16Kx16K. If arrays with larger pixels are available, the total number of arrays required is lower. The astronomer may wish to bin the CCDs in either the spectral or in the spatial dimensions to reduce the storage requirements for the data set. The detector system, therefore, is comparable in complexity to the NOAO Mosaic camera and similar

arrays in common use today.

Since the pixel sizes of current IR detectors are $\approx 18\mu$m for HgCdTe and $\approx 25-27\mu$m for InSb, fewer pixels are required to cover the focal surface than in the case of CCDs. Assuming large format arrays with 27μm pixels are available, we plan to use 16 arrays of 2Kx2K (mosaicked to 8Kx8K) for each spectrograph channel. The detector technology at near-IR wavelengths is technology driven at present, but the need for detectors for NGST and other ground-based facilities should result in usable detectors on the timescale of SWIFT.

5.6. Software

A diverse set of software is required for SWIFT: from observing preparation, through data taking, reduction, analysis, and archiving. Most of the basic data-reduction tools already exist to a large extent in current software packages (e.g., IRAF, SDSS), but they will need to be interfaced into an end-to-end system. However, the extreme number of spectra obtained per observation poses an exciting analysis challenge: the creation of "expert" software to perform preliminary data analysis screening. These might include identification of stellar and galaxy spectra (e.g., via principal component methods or neural networks); an automated stellar atmosphere modeling package to classify, measure velocities, and derive abundances for 10^5 stars while also flagging those spectra that do not resemble stars; discovery tools to maximize the extraction and classification of faint, serendipitously detected objects. These spectra may represent the truly fascinating serendipitous discoveries that must not be overlooked in the crush of a fully automated analysis pipeline.

5.7. Technical Challenges

5.7.1. Slit-Mask Technology

One of the major technical challenges is the efficient production of high quality slitmasks in order to maximize the use of SWIFT's highly multiplexed spectroscopic capability. Since it takes many hours to drill, punch, or burn (with a laser) many thousands of slitlets or holes in a mask, alternatives must be considered. Among these are "microshutters", LCD panels, and chemical etching. A fallback is to utilize a bank of several mask cutters of a more classical design in order to multiplex the mask generation. Furthermore, slitmasks must be astrometrically accurate over a half-meter curved focal surface. One possible solution is to coat a glass plate with a black substance and then "burn" off that substance with a laser

in the slitlet locations. In addition, since a large field of view causes atmospheric refractive effects that alter the apparent astrometry, a mask can be used for only a limited time on the sky unless the atmospheric distortion is optically corrected in the telescope. We are looking into ways to minimize this effect.

5.7.2. Scattered Light Reduction

Since scattered OH sky emission can significantly reduce the detected signal-to-noise ratio of faint targets in the near-IR, it is critical to minimize scattering sources in the instrument. VPH gratings typically produce less scattered light due to the lack of ruling errors and grating flaws which are sources of scattering in ruled, surface-relief gratings. In addition to paying close attention to anti-reflection coatings and glass quality, we will also explore some developing technologies (e.g., Rugate filters and spectral-hole burning filters) which might be capable of filtering out much of the OH contamination. Such technologies could be retrofitted if and when they become viable.

5.7.3. Adaptive Optics

It will be possible to consider incorporating in SWIFT a level of adaptive correction for correlated image motion (due to drive errors and telescope vibrations). We will also investigate higher-order adaptive correction for low altitude turbulence (Chun et al, 1998) which correlates well over an extended field. The very large corrected field of SWIFT, offering access to a number of bright stars in almost any observation, will be a significant advantage in wavefront analysis for partial, wide-field adaptive correction. The baseline budget below does not include adaptive correction.

5.8. A Rough Cost Estimate

Most aspects of the SWIFT project can be costed with reasonable accuracy based on existing facilities. Since we assume that no technological breakthroughs are achieved, the estimates below are conservative.

1. $50M – The fore-optic and enclosure: a relatively simple 8.4-m telescope that includes primary and secondary, mirror cells, telescope structure, control system, dome, and building. The cost basis derives from Gemini, Magellan, LBT, and the 3DT.

2. $4M – the 1.1-m corrector which includes the ADC, cells, and control system. The cost basis derives from the cost of the recently installed CTIO corrector (0.49-m), increased by diameter cubed.

3. $16M – the 4 spectrographs at $4M each, including the collimator, camera, and 3 gratings for resolutions of 500, 5000 and 20,000. The cost basis assumes that the similarly specified but somewhat smaller 4-m version will be $3M plus detectors.

4. $12M – Optical detector systems, consisting of 4 mosaics at $3M each, including per mosaic, 32 CCDs (2Kx4K), 8 controllers, a dewar, window, and shutter. The cost basis is from the 2 NOAO CCD Mosaic imagers.

5. $20M – IR detectors consisting of 4 mosaics at $4M each including per channel, 16 2Kx2K arrays, plus controllers. The cost basis is the current rate for a 2Kx2K array at $0.25M.

6. $1M – Instrument computers: 8 are required for data acquisition at $10K each, including storage for DVD or other media to archive the data. Since the integrations are fairly long at faint flux levels, the data rate is expected to be ∼50 Gbytes per night, which is not very high by tomorrow's standards. The cost basis is from existing Mosaic computers, and the continuing decline in the cost of computer hardware.

7. $6M – Software – includes data acquisiton, pipeline reduction and archiving. The cost is based on the other large scale software projects at NOAO (the IRAF project integrated over its entire 15 year lifetime totals ∼$5M in 1999 dollars). Much of the software, including some database and mining tools, could build on the legacy from the SDSS and the STScI archive. Further, we expect that external, diverse sources of funding will be available for the development of sophisticated "expert" software for higher level analyses, and we intend to team with external organizations in integrating the software into an accessible analysis package. The cost estimate reflects this expectation.

Thus, the total estimated construction cost for the SWIFT system — telescope, instrument, and software pipeline — is $109M. Operations for an integrated spectroscopic facility are relatively inexpensive: we estimate approximately 15 FTEs will be needed to support SWIFT. Except for the spectrograph costs, the other items are fairly secure and conservative. Obviously, technology breakthroughs may reduce this cost significantly and can be expected in the areas of the telescope, detectors, and software.

We would like to thank Paul Harding, Katherine Johnston, Guinevere Kaufmann, Rob Kennicutt, Anatoly Klypin, Karl Glazebrook, James Graham, Marguerite Pierre, Phil Pinto, Marc Postman, Michael Rich, Gary Schmidt, Alex Szalay, Rosie Wyse, and Naoki Yoshida for figures and ideas that contributed to this document. This document was prepared with considerable assistance from the NOAO staff, including Taft Armandroff, Ian Dell'Antonio, Jack Baldwin, Dave De Young, Jay Elias, Mark Giampapa, Richard Green Buell Jannuzi, Dick Joyce, Tod Lauer, Roger Lynds, Mike Merrill, Knut Olsen, Caty Pilachowski, Ron Probst, James Rhoads, Steve Ridgway, Bob Schommer, Nigel Sharp, Steve Strom, Nick Suntzeff, Glenn Tiede, Jeff Valenti, and Sidney Wolff.